5-1-2023

Temperature-controlled transition boiling at the stagnation zone during submerged jet impingement of a dielectric fluid

T. Stamps

Justin A. Weibel
jaweibel@purdue.edu

2023 22nd IEEE Intersociety Conference on Thermal and Thermomechanical Phenomena in Electronic Systems (ITherm) | 979-8-3503-2166-1/23/$31.00 ©2023 IEEE | DOI: 10.1109/ITHERM55368.2023.10177543

Temperature-Controlled Transition Boiling at the Stagnation Zone during Submerged Jet Impingement of a Dielectric Fluid

Tyler Stamps, Justin A. Weibel
Cooling Technologies Research Center
School of Mechanical Engineering, Purdue University
West Lafayette, IN 47907 USA
Email: jaweibel@purdue.edu

***Abstract*—Two-phase jet impingement offers high heat transfer coefficients suitable for thermal management in applications ranging from metals processing to electronics cooling. Most prior fundamental studies focus on heat-flux-controlled nucleate boiling up to the critical heat flux (CHF). There has been comparatively little investigation of two-phase jet impingement under surface-temperature-controlled conditions, despite applications that impose heating conditions that lie between the extremes of prescribed flux versus temperature. Exploring boiling regimes that occur during temperature-controlled conditions is important to understand the design space. In particular, two-phase jet impingement differs from pool boiling in the transition boiling regime. Impingement of subcooled liquid rewets the surface, thereby delaying the start of complete film boiling in the stagnation zone. As the surface temperature increases, the heat flux dissipated is relatively constant, forming a so-called "shoulder" on the boiling curve. Prior studies of this shoulder effect exclusively use water as the working fluid. In this study, temperature-controlled submerged jet impingement is experimentally characterized using the dielectric liquid HFE-7100. A single 3 mm-diameter jet orifice impinges on a 9.8 mm-diameter circular copper heater surface covered by the jet stagnation zone. The shoulder effect is observed by incrementing the surface superheat in the transition regime using a PID controller. The boiling data are supplemented by high-speed imaging to relate the flow phenomena observed in the confinement gap to the temperature-controlled boiling curve performance.**

Keywords— Jet impingement, two-phase heat transfer, transition boiling, electronics cooling

I. INTRODUCTION

Two-phase jet impingement is an effective thermal management technique for cooling local hotspots and high-density electronic systems. As for all boiling processes, the nucleate boiling regime during two-phase jet impingement occurs over a narrow surface temperature range, at a small superheat over the saturation temperature, due to the extremely effective transport processes. Heat flux is dissipated by convection and sensible heat of the liquid, as well as by latent heat via liquid-to-vapor phase change. Vapor thus generated is carried away from the heated surface by buoyancy and due to the inertia of the incoming jet. At some surface superheat, there is a maximum heat flux (q_{max}) at which nucleate boiling can be sustained before the boiling transitions to a different mode.

Design practices considering the classical boiling curve [1] (i.e., in a quiescent pool of saturated liquid) typically avoid operation at surface superheats near the point of maximum heat flux. This is because, under a surface heat-flux-controlled scenario, this value presents a critical heat flux (CHF) [2] that leads to film boiling when exceeded. Vapor coverage and insulation of the surface during film boiling at such high heat fluxes causes an instantaneous and significant increase in the surface temperature. Under temperature-controlled scenarios, increasing the surface superheat past the point of maximum heat flux incurs greatly reduce performance associated with the transition boiling regime during which there are unsteady fluctuations between nucleate and film boiling. Transition boiling curves are often simplified as a linear path [3] between CHF and the minimum film boiling point because the mechanisms are not well understood.

However, during subcooled two-phase jet impingement on a temperature-controlled surface, it has been observed that the formation of a vapor film is disrupted by the inertia of the subcooled jet in the stagnation zone directly under the jet orifice. This reshapes the boiling curve and causes the transition regime performance to be characterized by a constant "shoulder" heat flux (q_{sh}) over a wide temperature range [4-6]. A sketch of a temperature-controlled subcooled jet impingement boiling curve, with a shoulder heat flux in the transition boiling region, compared to a classical pool boiling curve is shown in Fig. 1. The shoulder heat flux value lies between the maximum nucleate boiling heat flux and classical transition boiling regime performance and has been observed to be at a higher value with increasing jet subcooling [6].

Investigation of temperature-controlled two-phase jet impingement has been previously investigated primarily owing to its important role in metals processing, as well as interest in other thermal management applications for which the boundary conditions are not well-represented by the canonical extreme of a prescribed heat flux. The first such steady-state experiments were performed by Robidou et al. [4, 5] using a free 1 × 9 mm slot jet of water with a subcooling of 16 K. They measured the

shoulder heat flux variation as a function of the distance from the stagnation zone using eight independently heated 10 × 10 mm copper modules which could reach up to 700°C, covering the full extent of the boiling curve up to film boiling. They observed that the transition jet-impingement boiling curves outside of the stagnation zone are close in shape to a pool boiling curve. These studies were followed by the work of Seiler-Marie et al. [6], who offered a physical explanation for the phenomenon, assuming the periodic bubble oscillations on the surface are driven by jet hydrodynamic fragmentation. One key observation of their study was that the shoulder heat flux during transition boiling is proportional to the inlet subcooling. Based on this observation, these authors proposed that heat transport in the shoulder region is characterized by a Rayleigh-Taylor instability between the liquid and vapor at the surface. Sensible heating of the subcooled liquid dissipates most of the energy which is then ejected into the surroundings by the bubble growth and jet inertia. The shoulder heat flux is hypothesized to be a constant value for this reason; vaporization contributes very little to this process, so the flux is capped after the sensible heat is fully utilized. By combining relations for the Rayleigh-Taylor instability frequency and critical wavelength with the flow rate of heated liquid displaced by each bubble, an equation for shoulder heat flux (q_{sh}) was derived [6]:

$$q_{sh} = K' \rho_l (\rho_l - \rho_v)^{-1/4} \sigma^{1/4} C_{pl} \Delta T_{sub} V_j^{1/2} D^{-1/4} \quad (1)$$

where ρ_l and ρ_v are the liquid and vapor densities, respectively, σ is the surface tension of the fluid, C_{pl} is the liquid specific heat, ΔT_{sub} is the degree of inlet subcooling, V_j is the jet velocity, D is the orifice diameter, and K' is an empirical coefficient found as 0.15 by fitting to data for a free water jet.

Owing to the typical application of metals quenching, all prior studies of this shoulder heat flux in the temperature-controlled transition boiling curve use unconfined free jets with water as the working fluid [7]. For other compact thermal management applications, refrigerants and dielectric fluids are needed, potentially in submerged jet impingement

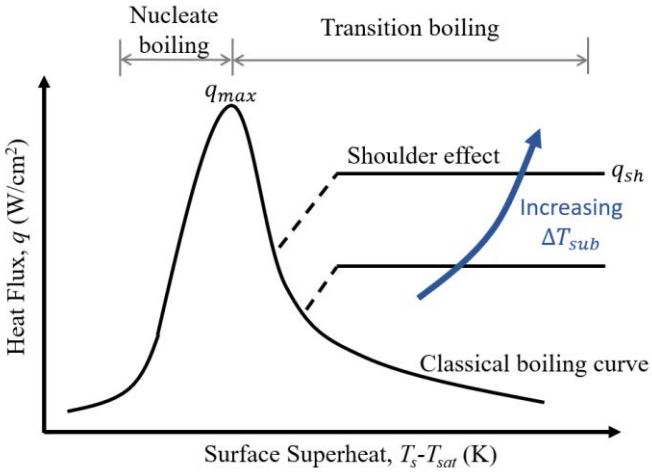

Fig. 1. Sketch of temperature-controlled two-phase jet impingement boiling curve at different inlet subcooling levels overlaid on a classical pool boiling curve.

configurations, all of which have not been previously considered for this scarcely investigated shoulder effect region. Our current study demonstrates the occurrence of the shoulder heat flux region for submerged, subcooled two-phase jet impingement of a dielectric working fluid on a temperature-controlled surface. The heat transfer data are supplemented by high-speed visualization and the measured shoulder heat fluxes values are compared against the predictions of an available correlation from the literature.

II. Experimental Methods

A. Experimental Facility

Jet impingement experiments were performed using the dielectric fluid HFE-7100. The flow loop was fully described previously in [8] with the addition of a clear inlet plenum modified from that of [9] to allow top-down high speed visualization of the boiling surface. The flow loop connects to a jet impingement test chamber, shown in the photograph in Fig. 2, with a jet orifice plater, heater sample, and surface temperature controller that were newly developed for this work.

To briefly summarize the flow loop, the working fluid is pumped from a reservoir to the experimental chamber using a gear pump. A liquid-to-air heat exchanger placed before the pump sets the inlet subcooling to the chamber by setting the fan speed. Fine-tuning of subcooling is supplemented by an inline preheater just before the chamber. Testing is performed at two different subcoolings (ΔT_{sub}) of 5 K and 15 K below the saturation temperature of HFE-7100 (T_{sat} = 61°C, operating at atmospheric pressure). Flow enters into the test chamber through a plenum that has a flow distributor to neutralize any entrance effects before directing liquid to the orifice that forms the jet which impinges onto the heated surface. The plenum and orifice plate are made from polycarbonate for top-down visualization.

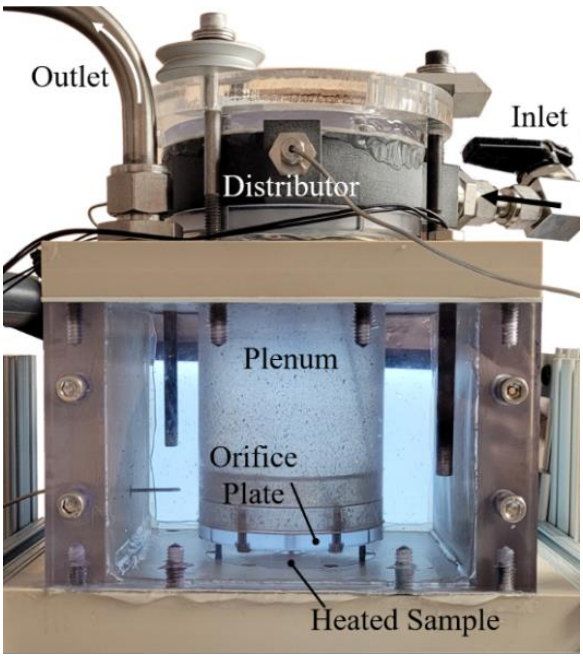

Fig. 2. Photograph of the jet impingement boiling facility test chamber with key components labeled.

The flow leaving the jet then escapes into the surrounding chamber, made from polyether ether ketone (PEEK) with polycarbonate windows for side-view visualization. Finally, the flow reaches the chamber outlet and flows back to the reservoir. Three Graham condensers are mounted above the reservoir to condense the vapor generated by boiling.

The jet impingement geometry, operating conditions, and heater characteristics are chosen specifically to probe the shoulder heat flux phenomenon during transition boiling. In particular, the following guidelines [10] are used to ensure that the sample surface is covered by the stagnation zone where this phenomenon is reported to occur. For a circular submerged jet, the stagnation zone has an area of approximately 1.6 to 3 orifice diameters. For this experiment, the 6.35-mm thick orifice plate hosts a single D = 3 mm orifice, which creates a V_j = 3 m/s jet (1.27 L/min) directed at a 9.8 mm diameter target surface. Furthermore, a submerged jet entrains the surrounding fluid and loses coherence with increasing height from the surface. For this reason, the jet height-to-orifice diameter ratio (H/D) must be less than 5 so that the orifice jet velocity persists to the target surface [10]. Spacer pins are installed between the orifice plate and the sample holder plate to precisely set the desired jet height to H = 7.5 mm above the heater surface.

Three vertical T-type thermocouple rakes are spread evenly in the copper heater block, which allows the calculation of the heat flux and surface temperature from the measured temperature gradient and known block thermal conductivity. The center rake has four thermocouples spaced 2.0 mm, 5.5 mm, 9.0 mm, and 12.5 mm below the top surface. The front and back rakes have two thermocouples each and are spaced 1.9 mm from the edge, with one positioned 2.0 mm below the surface and the other located 12.5 mm from the surface. The heater block has four 100 W cartridge heaters that can be either powered to a set wattage or allow PID control of the surface temperature. The PID controller, implemented in LabVIEW, outputs the heater power as a function of the instantaneous surface temperature extrapolated from the thermocouple rakes, to reach some setpoint temperature. To verify the controller operation, it was confirmed that there was no measurable difference between heat-flux-controlled and temperature-controlled boiling performance in the nucleate boiling region. The measured temperature data are supplemented by high-speed visualization (Phantom VEO 710L) from the available top and side views.

B. Test Procedure

The fluid is vigorously boiled for at least two hours to degas before each experiment and kept saturated in the reservoir throughout the test. During degassing, the condensers are open to the environment and allow non-condensable gases to escape the system. In each experiment, the nucleate boiling region is traversed under a heat-flux-controlled mode by incrementing the power in steps of 4-10 W and allowing it to reach steady state, where the surface temperature changes at a rate less than 1 K/hr. The resultant temperature and corresponding heat flux were recorded as an average over 2 min at a sensor polling rate of 0.5 Hz. This procedure is followed up to the maximum heat flux (q_{max}), where either critical heat flux will occur or transition boiling will begin, depending on the mode of control.

To enter the transition boiling regime, the heater power is manually increased to slightly exceed the superheat at the maximum heat flux whereupon the PID controller is immediately engaged. The PID temperature setpoint is then increased in 10 K increments up to 220°C, near the maximum service temperature of the PEEK sample holding plate. We note that temperature control in the transition boiling shoulder region is challenging because the boiling curve slope is nearly flat, i.e., the heat flux is insensitive to temperature. The PID control scheme, therefore, struggles to lock at a steady setpoint surface temperature even after extensive tuning of the controller. Nevertheless, the controller manages to bound any oscillations in surface temperature within ±5 K of the setpoint. The delivered heater power is integrated over the timespan to find an average heat flux. Temperature data acquired in this region are plotted with error bars that indicate the span of oscillations around the setpoint and the associated time-averaged heat flux.

III. Results

The measured heat flux as a function of the surface superheat (T_s - T_{sat}) along the nucleate and transition boiling regions are shown in Fig. 3 for the two different subcooling values tested. The curves begin with a shallow slope associated with single-phase jet impingement, before nucleate boiling begins and the curves turn sharply upward. Nucleate boiling continues until the process approaches the maximum heat flux, where the slope begins to flatten. There is then a jump in temperature upon entering the transition regime and observing the shoulder heat flux phenomenon. This jump is related to the manual switch from flux-controlled to temperature-controlled heating; set temperatures in this range are uncontrollable and drift up to higher temperatures in the shoulder region. Further refinement of the surface temperature control method is needed to identify state points between the maximum heat flux and shoulder region, thus characterizing the temperature at which the shoulder effect begins. Once in the shoulder region, the slope in the boiling curve is nearly flat, and the average flux across all data is used to calculate the value of q_{sh} for each subcooling case.

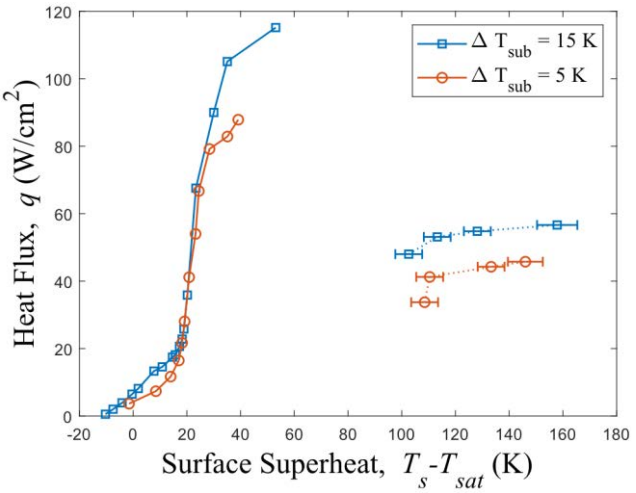

Fig. 3. Measured temperature-controlled two-phase jet impingement boiling curve for 5 K and 15 K inlet subcooling with V_j = 3 m/s, D = 3 mm, H = 7.5 mm.

The shoulder heat flux is still a significant fraction of q_{max} and much higher than pool boiling would be expected to dissipate at the same superheat. This measurement is confirmation that the shoulder effect is present for a submerged jet of dielectric fluid.

Representative images extracted from high-speed visualization of boiling during the nucleate and transition regimes are shown in Fig. 4 (top view) and Fig. 5 (side view). The blue traces outline instantaneous vapor locations, to enhance visibility in the static images. Bubble generation occurs at a very high frequency during transition boiling, requiring recording at 50,000 frames per second to capture the rapid movement. From the high-speed visualizations, it is evident that the transition boiling regime has less voluminous bubbles compared to the nucleate regime. In the video, the transition bubbles are generated and condensed into the surrounding fluid at a faster rate than the nucleate bubbles and there is no visible vapor layer on the surface of the sample.

The effect of the degree of subcooling, ΔT_{sub}, on the shoulder heat flux is highlighted by Fig. 3. Prior to the transition boiling region, a higher subcooling led to a higher maximum heat flux (q_{max}) of 87.9 W/cm^2 at 5 K versus 115.6 W/cm^2 at 15 K. After transition, the shoulder heat flux (q_{max}) has a similar relative difference of 40.9 W/cm^2 versus 52.8 W/cm^2, where a higher subcooling increases the shoulder heat flux as previously observed in the literature for free water jets [4-7].

We compare our measured shoulder heat fluxes with q_{sh} values predicted using Eq. 1. All parameters input into this relation are taken from the current experimental geometries, operating conditions, and working fluid properties, except for the empirical constant set to K'=0.15 as previously fitted in the literature [6] for free water jets. With these inputs, the values of q_{sh} estimated are 47.8 W/cm^2 and 143.5 W/cm^2 for 5 K and 15 K, respectively. While the mismatch in magnitude at a given subcooling can be attributed to the choice of fitting constant K', a more notable difference is that the relation in Eq. 1 predicts a linear correlation with the degree of subcooling. This relatively modest increase in the shoulder heat flux by only 27% with a tripling of the inlet subcooling differs from our observations, for which, the shoulder heat flux instead appears to be a constant fraction of the maximum heat flux, 46.5% and 45.6%, for 5 K and 15 K, respectively. To add confidence to the current measurements, the maximum heat fluxes are also compared to an accepted expression for the critical heat flux of a saturated jet by

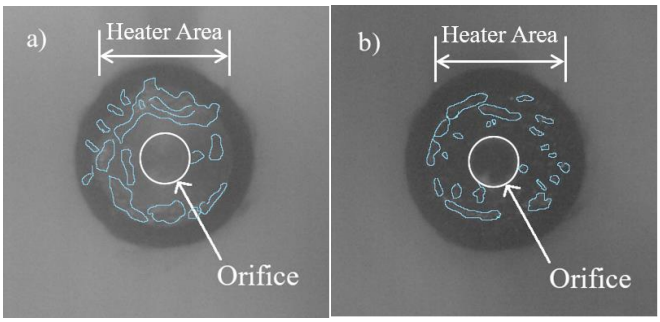

Fig. 4. Image frames of the sample top-down view, extracted from high-speed visualizations captured at 50,000 fps, the a) nucleate boiling and b) transition boiling regimes. The blue traces outline the instantaneous bubble position.

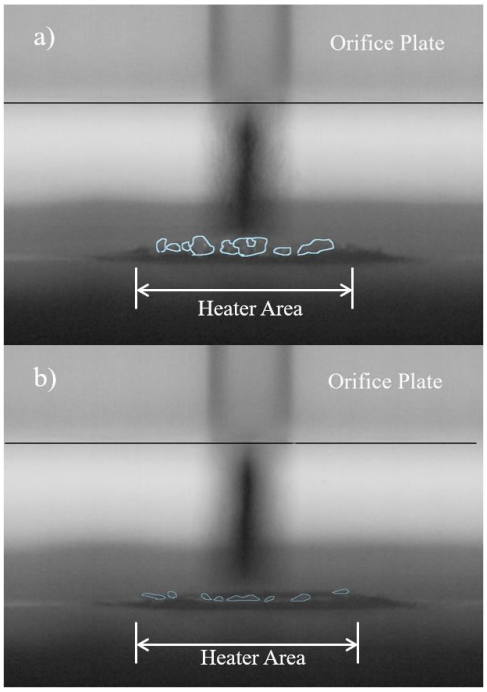

Fig. 5. Image frames of the sample side view, extracted from high-speed visualizations captured at 50,000 fps, the a) nucleate boiling and b) transition boiling regimes. The blue traces outline the instantaneous bubble position.

Katto and Yokoya [11]; the two measurements here are within 22% of the prediction q_{max} = 96.3 W/cm^2. Given the sparse literature data available in the shoulder heat flux region from which these comparisons are drawn, these behavior differences can be easily attributed to numerous possible factors including the fluid type, submerged configuration, and extent of the stagnation zone, to name a few. This highlights the need for future work to develop more comprehensive tools for the prediction of shoulder heat flux as a function of the jet geometry, operating characteristics, and fluid type.

IV. Conclusions

This work demonstrates that the temperature-controlled transition boiling shoulder effect is present for jet impingement of the dielectric fluid HFE-7100. Prior work in the literature revealed this shoulder heat flux effect for free jet impingement of water. While the general behavior in this regime is consistent with these past observations, as confirmed via high-speed visualization, the trend in the shoulder heat flux values with inlet subcooling seems to differ under the current submerged jet configuration. Future work must further investigate the influence of variations in jet geometry, velocity, and subcooling on the shoulder effect and heat flux.

References

[1] J. M. Ramilison and J. H. Lienhard, "Transition Boiling Heat Transfer and the Film Transition Regime," Journal of Heat Transfer, vol. 109, no. 3, pp. 746–752, Aug. 1987, doi: 10.1115/1.3248153.

[2] V. S. Devahdhanush and I. Mudawar, "Review of Critical Heat Flux (CHF) in Jet Impingement Boiling," International Journal of Heat and Mass Transfer, vol. 169, p. 120893, Apr. 2021, doi: 10.1016/j.ijheatmasstransfer.2020.120893.

[3] M. Winter and J. A. Weibel, "The Effect of Fin Array Height and Spacing on Heat Transfer Performance during Pool Boiling from Extended

Surfaces," in the 21st IEEE Intersociety Conference on Thermal and Thermomechanical Phenomena in Electronic Systems (ITherm), San Diego, CA, USA, May 2022, pp. 1–7. doi: 10.1109/iTherm54085.2022.9899575.

[4] H. Robidou, H. Auracher, P. Gardin, and M. Lebouché, "Controlled Cooling of a Hot Plate with a Water Jet," Experimental Thermal and Fluid Science, vol. 26, no. 2–4, pp. 123–129, Jun. 2002, doi: 10.1016/S0894-1777(02)00118-8.

[5] H. Robidou, H. Auracher, P. Gardin, M. Lebouché, and L. Bogdanic, "Local Heat Transfer from a Hot Plate to a Water Jet," Heat and Mass Transfer, vol. 39, no. 10, pp. 861–867, Nov. 2003, doi: 10.1007/s00231-002-0335-6.

[6] N. Seiler-Marie, J.-M. Seiler, and O. Simonin, "Transition Boiling at Jet Impingement," International Journal of Heat and Mass Transfer, vol. 47, no. 23, pp. 5059–5070, Nov. 2004, doi: 10.1016/j.ijheatmasstransfer.2004.06.009.

[7] C. Agrawal, "Surface Quenching by Jet Impingement − A Review," steel research international., vol. 90, no. 1, p. 1800285, Jan. 2019, doi: 10.1002/srin.201800285.

[8] M. D. Clark, J. A. Weibel, and S. V. Garimella, "Identification of Nucleate Boiling as the Dominant Heat Transfer Mechanism during Confined Two-Phase Jet Impingement," International Journal of Heat and Mass Transfer, vol. 128, pp. 1095–1101, Jan. 2019, doi: 10.1016/j.ijheatmasstransfer.2018.09.058.

[9] C. Mira-Hernández, J. A. Weibel, and S. V. Garimella, "Visualizing Near-Wall Two-Phase Flow Morphology during Confined and Submerged Jet Impingement Boiling to the Point of Critical Heat Flux," International Journal of Heat and Mass Transfer, vol. 142, p. 118407, Oct. 2019, doi: 10.1016/j.ijheatmasstransfer.2019.07.057.

[10] F. P. Incropera, Liquid Cooling of Electronic Devices by Single-Phase Convection, vol. 3. Wiley-Interscience, 1999.

[11] Y. Katto and S. Yokoya, "Critical Heat Flux on a Disk Heater Cooled by a Circular Jet of Saturated Liquid Impinging at the Center," International Journal of Heat and Mass Transfer, vol. 31, no. 2, pp. 219–227, Feb. 1988, doi: 10.1016/0017-9310(88)90003-8